Fast-ion energy loss during TAE avalanches in the National Spherical Torus Experiment

E. D. Fredrickson, N. A. Crocker[1], D. Darrow, N. N. Gorelenkov, G. Kramer, S. Kubota[1], M. Podesta, A. Bortolon[2], S. Gerhardt, R. E. Bell, A. Diallo, B. LeBlanc, F. M. Levinton[3], R. White, H. Yuh[3]

Princeton Plasma Physics Laboratory, Princeton New Jersey 08543
[1]Univ. of California, Los Angeles, CA 90095
[2]Univ. of California., Irvine, CA 92697
[3]Nova Photonics, Princeton, NJ 08543

email contact of main author: efredrickson@pppl.gov

Abstract. Strong TAE avalanches on NSTX, the National Spherical Torus Experiment are typically correlated with drops in the neutron rate in the range of 5% - 15%. In previous studies of avalanches in L-mode plasmas, these neutron drops were found to be consistent with modeled losses of fast ions. Here we expand the study to TAE avalanches in NSTX H-mode plasmas with improved analysis techniques. At the measured TAE amplitudes, simulations with the ORBIT code predict that fast ion losses are negligible. However, the simulations predict that the TAE scatter the fast ions in energy, resulting in a small (≈ 3-5 %) drop in fast ion β. The net decrease in energy of the fast ions and redistribution to regions of lower density is sufficient to account for most of the drop in neutron rate. This loss of energy from the fast ion population is comparable to the estimated energy lost by damping from the Alfvén wave during the burst.

1. Introduction

The ability to predict the confinement and energy transfer rate of fast ions to the thermal plasma is important for optimizing the performance of ITER and other tokamaks. The presence of TAE or other MHD could impair the accurate modeling of beam driven currents that ITER and ST's rely upon. In this paper we report that modeling of the effect of TAE on fast ions finds that diffusion of fast ions in real and phase space, resulting in a net drop in fast ion energy, explains the observed neutron rate drop, without the need for significant fast ion loss.

Fast ions on NSTX [1] are known to be redistributed by low frequency MHD (kinks, NTMs), energetic particle modes and TAE avalanches [2], affecting the beam-driven current profile [3]. Fast ion redistribution by avalanches has been successfully modeled in L-mode plasmas, using profile measurements of TAE amplitudes with a reflectometer array [4]. We have improved those analysis techniques and analyze avalanches in an H-mode plasma.

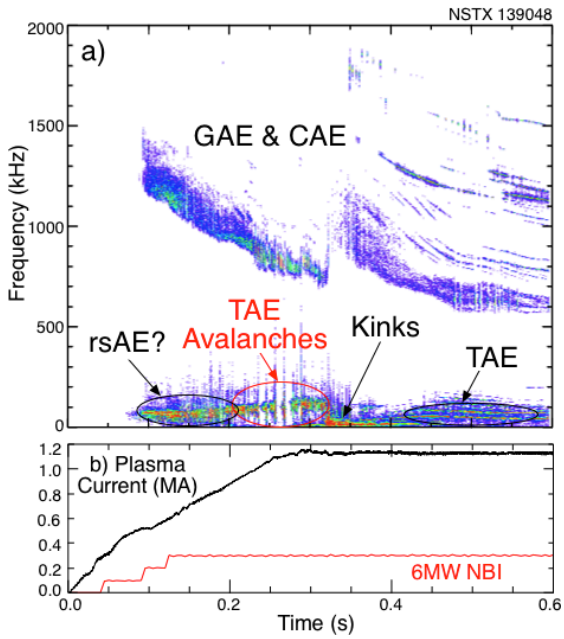

Fig. 1 a) spectrogram of magnetic fluctuations, b) Plasma current and neutral beam power evolution.

2. Experimental Observations

Here we look at a relatively low-density H-mode plasma with enough core density peaking for mode amplitude measurements with several reflectometer channels. The spectrogram of a Mirnov coil signal shown in Fig. 1a shows a fairly typical collection of fast ion driven instabilities for this shot. The plasma current and neutral beam power time dependence are shown in Fig. 1b. Instabilities identified as TAE avalanches appear, as indicated, between ≈ 0.2 s and ≈ 0.3 s. TAE avalanches are most commonly seen in this time window, possibly related to the relaxation of the current profile through a strongly shear-reversed state. Compressional and Global Alfvén eigenmodes are present at higher frequencies and may play a role in modifying the fast ion distribution function.

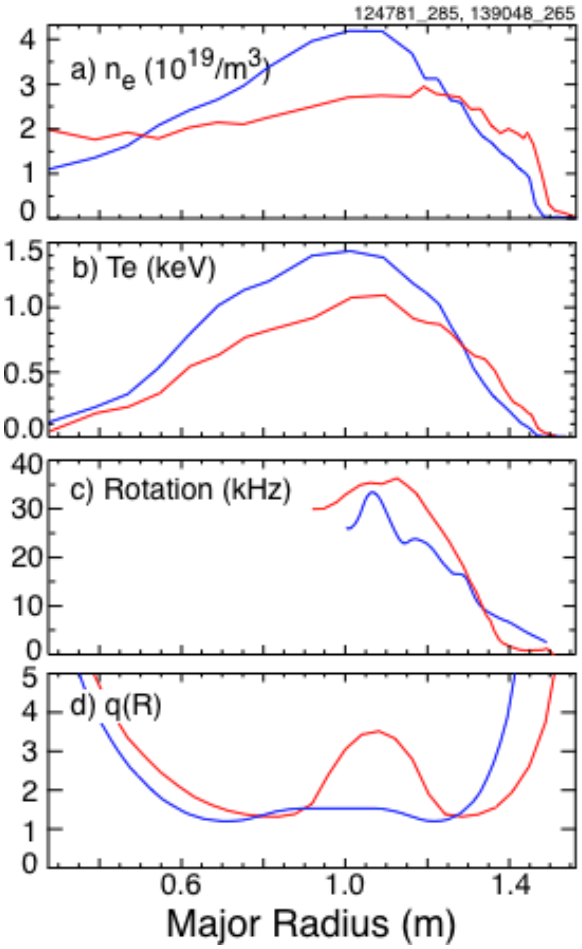

Fig. 2. Profiles of a) density, b) electron temperature, c) rotation velocity and d) q for the H-mode (red) and L-mode (blue).

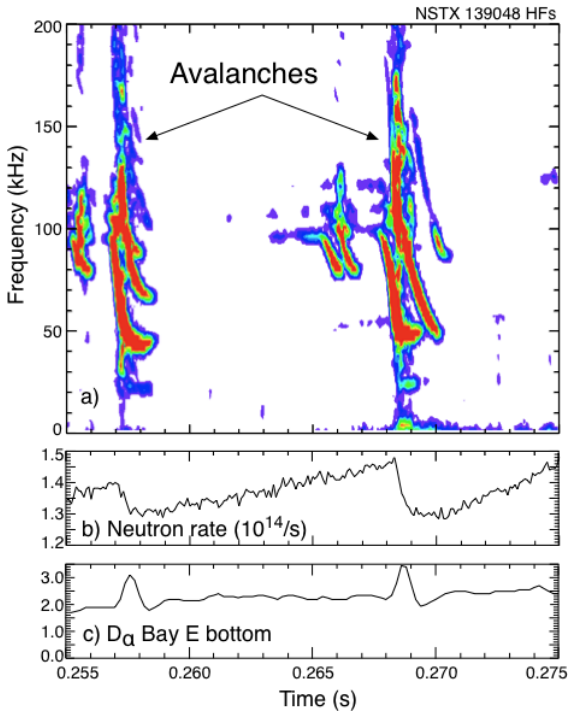

Fig. 3. a) a) Spectrogram of magnetic fluctuations showing two TAE avalanche bursts, b) neutron rate drops at each burst (note suppressed zero), c) D_α spikes at bursts.

The H-mode plasma studied here has a broader, less peaked density profile and more strongly reversed q profile than the L-mode shot analyzed earlier (Fig. 2a and Fig. 2d, respectively). These changes will have some affect on the TAE gap structure, but as will be seen, the dominant characteristics of the TAE gap structure on NSTX are set by the low aspect ratio and strong toroidal rotation (Fig. 2c). The distortion of the gap tends to 'close' the gap such that TAE intercept the continuum around the half-radius region.

The spectrogram of a Mirnov coil signal showing two of the TAE avalanches is shown in Fig. 3a. Coincident with the growth of multiple modes, there is a sharp drop in the neutron production rate (Fig. 3b) and a spike in D_α emission (Fig. 3c). The neutron rate drop and D_α spike together suggest the loss of at least some fast ions at this event. In the remainder of the paper we will discuss attempts to model the effect of

the TAE on the fast ion distribution function.

There are four important modes in this avalanche burst. The avalanche begins with the strong growth of an n=2 TAE which triggers n=4 and n=6 modes, and then an n=1 TAE. The amplitude evolutions of these four modes, as measured with three internal reflectometer channels, are shown in Fig. 4b. In both Figs. 4a and 4b, the solid curves are analytic approximations to the frequency and amplitude evolutions which are used in the ORBIT code [5] simulations described below.

3. NOVA and ORBIT simulations

The experimental measurements of the mode structure are insufficiently detailed to use in ORBIT simulations. Instead, we use the ideal code NOVA [6,7], together with the plasma equilibrium as input, to find the natural, linear eigenmodes for the reconstructed plasma equilibrium, and

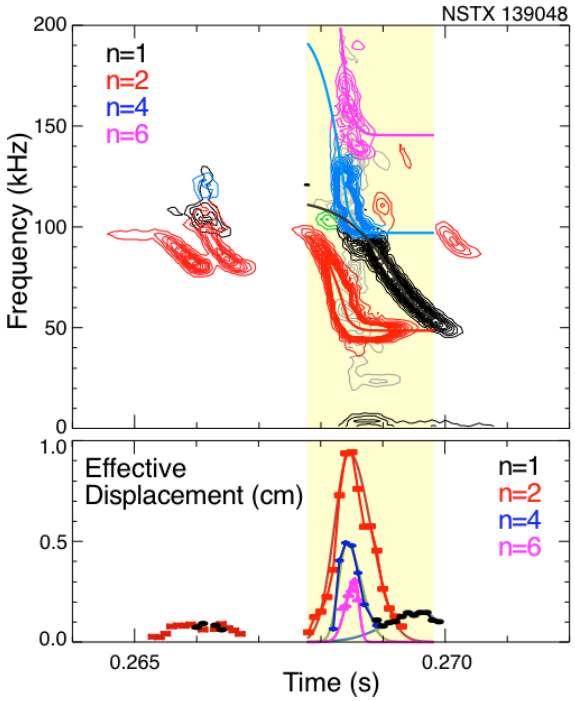

Fig. 4. a) Spectrogram of a Mirnov coil where contours are color-coded to indicate the toroidal mode numbers, as indicated in the legend, b) the peak mode amplitude evolution for each mode from the reflectometer array.

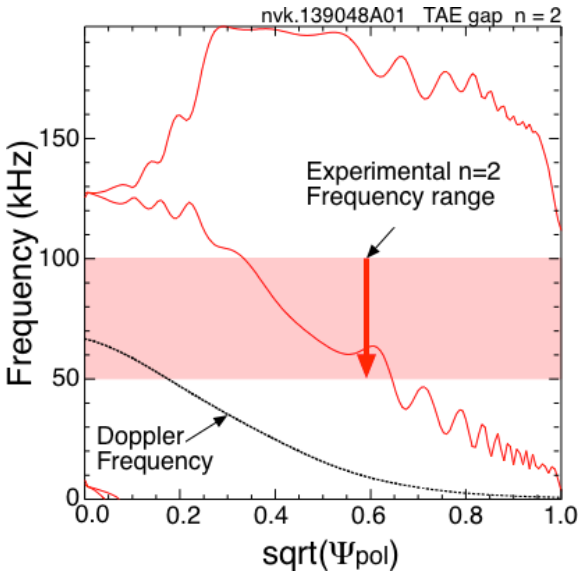

Fig. 5. The continuum structure for the n=2 TAE including the experimental sheared rotation profile. Red band shows range of the n=2 TAE frequency chirp.

choose from among them those that best match the reflectometer profile measurements. As NOVA is a linear code, we scale the eigenmodes so that the simulated reflectometer response matches the amplitude of the reflectometer signals. The experimental modes are clearly non-linear, with strong frequency chirping, so the experimental frequency evolutions are also used in ORBIT. Within experimental uncertainty the mode structure is not strongly changed during the burst so use of the linear modes is justified.

NOVA is an ideal code and there are poles in the equations at the continuum crossings that are not present with more complete physics models. Further, the eigenmodes in NOVA are necessarily represented with an incomplete set of poloidal harmonics due to the presence of the separatrix at the plasma edge. Finally, these NOVA used a conducting wall boundary condition at the plasma surface, whereas there is a fairly large gap between the last closed flux surface and the vacuum vessel walls or stabilizing plates. Thus, the NOVA eigenmodes should be regarded as only approximate representations of the

actual modes. For the ORBIT simulations, only the twelve largest poloidal harmonics from each mode were used.

The TAE gap profile and representative modes are shown in Figs. 5 and 6. The strong rotation distorts the gap profile and the first order effects of this are included in the NOVA eigenmode calculations. The reflectometer response is simulated using the NOVA eigenmodes (solid curve, Fig. 6) and compared to the reflectometer data (points with error bars in Fig. 6) to determine the absolute amplitude of each eigenmode.

Extensive ORBIT simulations suggest that the results are not particularly sensitive to detailed structure of the modes. For example, a simulation with just the n=2 mode alone accounts for about half of the neutron drop. This assumption of insensitivity to detailed mode structure is supported by experimental observations where the effect of the TAE avalanches on neutron rate is fairly robust while the

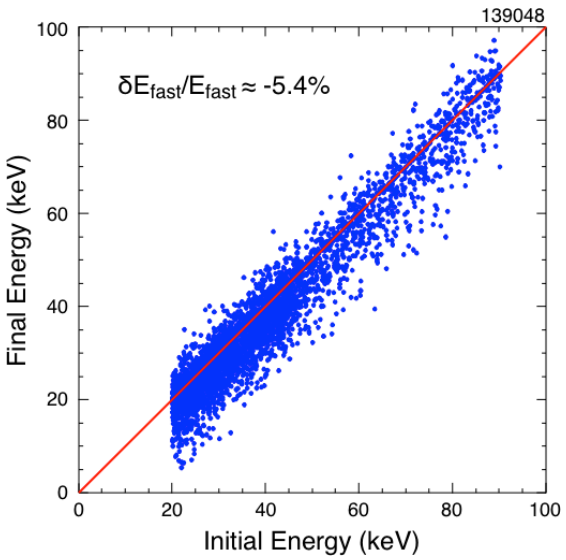

Fig. 7. Initial and final beam ion energies for an ORBIT simulation using measured mode amplitude and frequency evolutions.

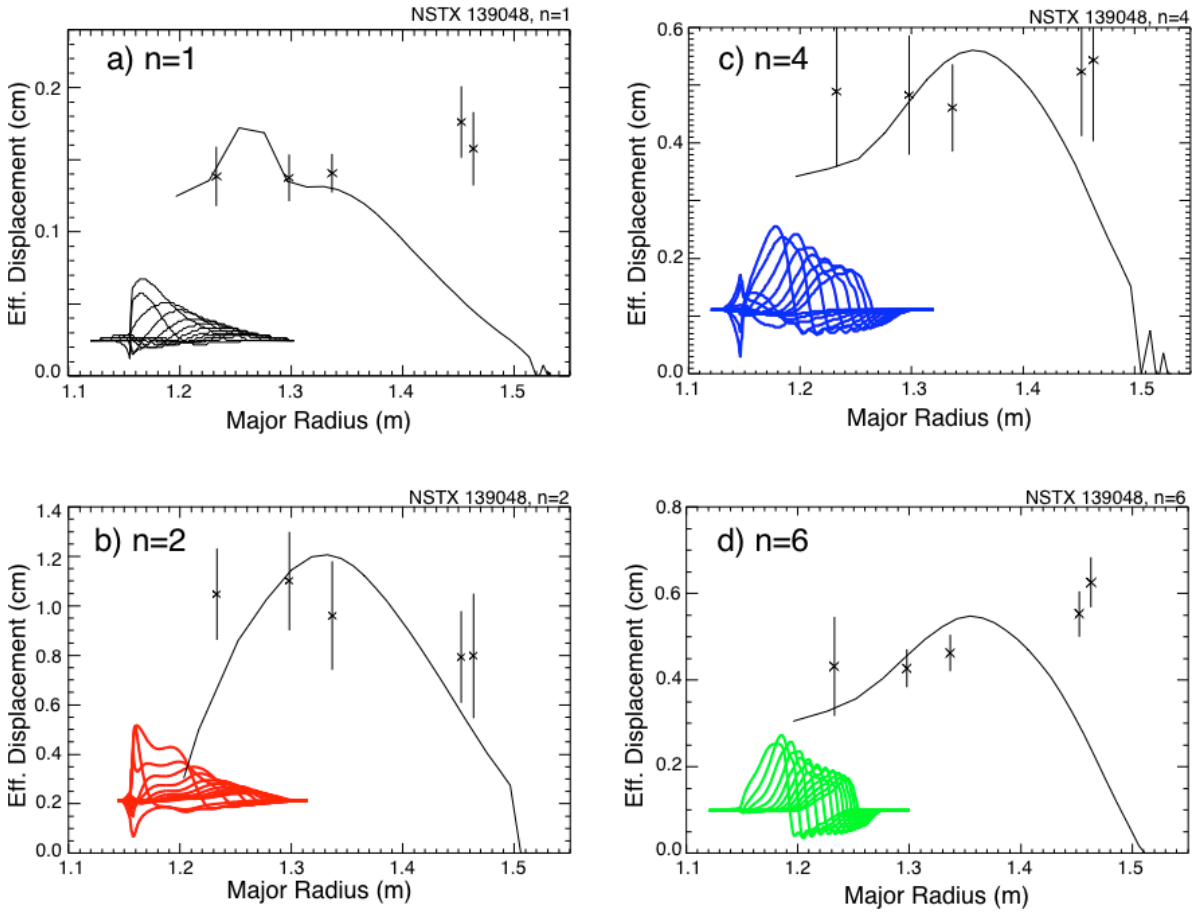

Fig. 6. Solid curves are simulated reflectometer response, points are reflectometer data, inset are NOVA poloidal harmonics for, a) n=1 mode, b) n=2 mode, c) n=4 mode and d) n=6 mode.

current profile, thus gap structure, shows substantial evolution.

Simulations with ORBIT find very small fast ion losses at the nominal measured mode amplitudes. The threshold for onset of fast ion losses is slightly higher than the measured mode amplitude. However, there is a change in the energy of the fast ions due to interactions with the multiple TAE at amplitudes lower than this. This is illustrated qualitatively in Fig. 7 where the final energy for each fast ion is plotted against its initial energy. The red line shows fast ions with essentially unchanged energy between the beginning and end of the simulation, but that doesn't necessarily mean that the energy was constant.

The change in energy of each fast ion, together with its change in radial position can be used to estimate the net change in neutron rate predicted by the ORBIT simulations. The change in beam-target reaction rate (≈74% of the total) can be estimated as the change in

$S_{B\text{-}T} \approx \Sigma n_d(\rho_n)\sigma(E_n)v_n$,

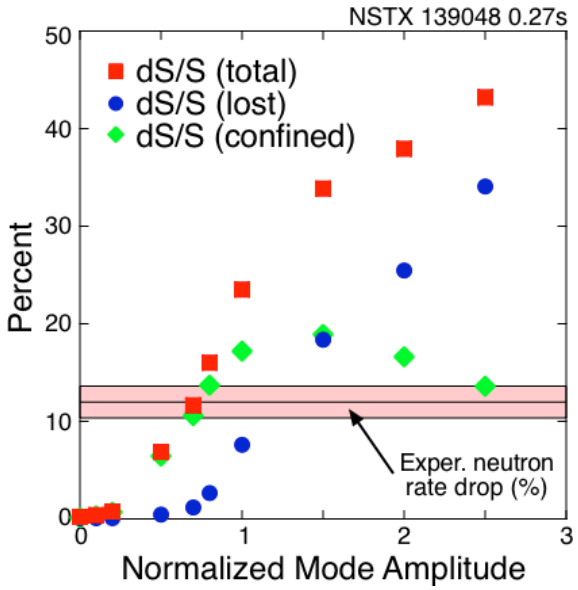

Fig. 8. Total neutron rate drop vs. scaled TAE amplitude (red squares), for the confined fast ion population (green diamonds) and due only to fast ion losses (blue circles).

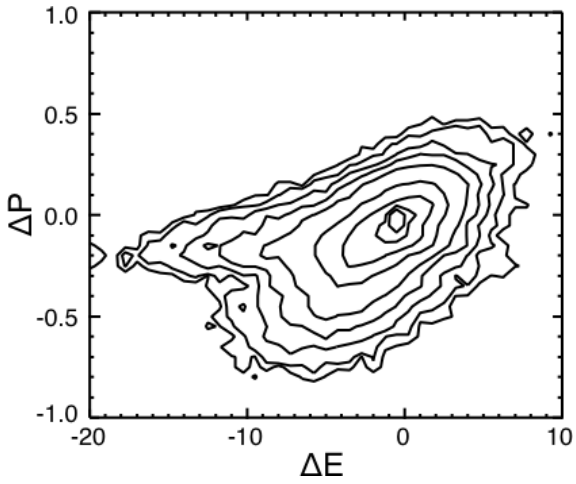

Fig. 9. Contour plot of the density of fast ions vs. change in canonical angular momentum (ΔP) and change in energy (ΔE).

where the sum is over the fast ion population and $n_d(\rho_n)$ is the local thermal deuterium density for each fast ion [8]. The change in beam-beam neutron rate (≈26% of the total neutron rate) is harder to calculate, but an estimate was made assuming a linear dependence on energy,

$S_{B\text{-}B} \approx \Sigma n_{fast}(\rho_n)E_n v_n$.

For a Maxwellian distribution with temperatures in the range 40 to 60 keV the neutron production increases roughly linearly with the temperature.

The total predicted neutron rate change from the energy drop, fast ion redistribution and fast ion loss is shown as the red points in Fig. 8, for various assumed mode amplitudes normalized to the experimental amplitude. The blue points show change in neutron rate from only fast ion losses. The measured neutron rate drop is roughly in agreement with the ORBIT simulations using 0.7 of the measured mode amplitudes. For this simulation, the bulk of the neutron rate drop is from energy loss (≈50%), redistribution (≈40%) with only ≈10% from fast ion losses. Both the fast ion energy losses and fast-ion losses show a threshold-like onset with mode amplitude, with the energy loss threshold onset at lower amplitude.

The ORBIT simulation using 0.7 of the measured mode amplitudes predicts a net drop in the total energy of the fast ions of ≈ 3.4%, and a drop in neutron rate of approximately 12%. The energy lost from the modes to the thermal plasma due to various damping mechanisms is proportional to the burst duration and the (uncertain) mode damping rates. Experimental estimates of the damping rate range from $\gamma_{damp}/\omega \approx 0.6\%$ to 1.6%, and NOVA-k predicts $\gamma_{damp}/\omega \approx 2.1\%$. Over this range, the estimated energy transferred from the TAE burst to the thermal plasma is 4-10 times the peak energy in the mode, or roughly 2.6% to 6.5% of the total energy in the fast ion population.

For a single mode the ion's canonical angular momentum and energy should satisfy the conservation relation, $nE - \omega P =$ const, or $dP/dE = n/\omega$ (where n in the toroidal mode number, P is the canonical angular momentum). For the TAE avalanches there are multiple n's present and of course the frequency is changing by approximately a factor of two. Nevertheless, there is some remnant of this conservation law present in the simulation data, as seen in Fig. 9. There is substantial broadening of the ΔP/ΔE relationship, but there remains a clear diagonal elongation of the contours. Here, ΔP and ΔE were calculated between the start and end of the simulation.

Of perhaps more interest is a plot showing which fast ions are most affected by the modes. To construct the data shown in Fig. 10b, the change in energy of each fast ion is recorded for each small time step in ORBIT. The rms(δE/δt) is calculated for each "bin" in the parameters μB/E and P. The data is only shown for one small energy range, and the figure will change for each different energy range. The larger the rms energy change, the more interaction the fast

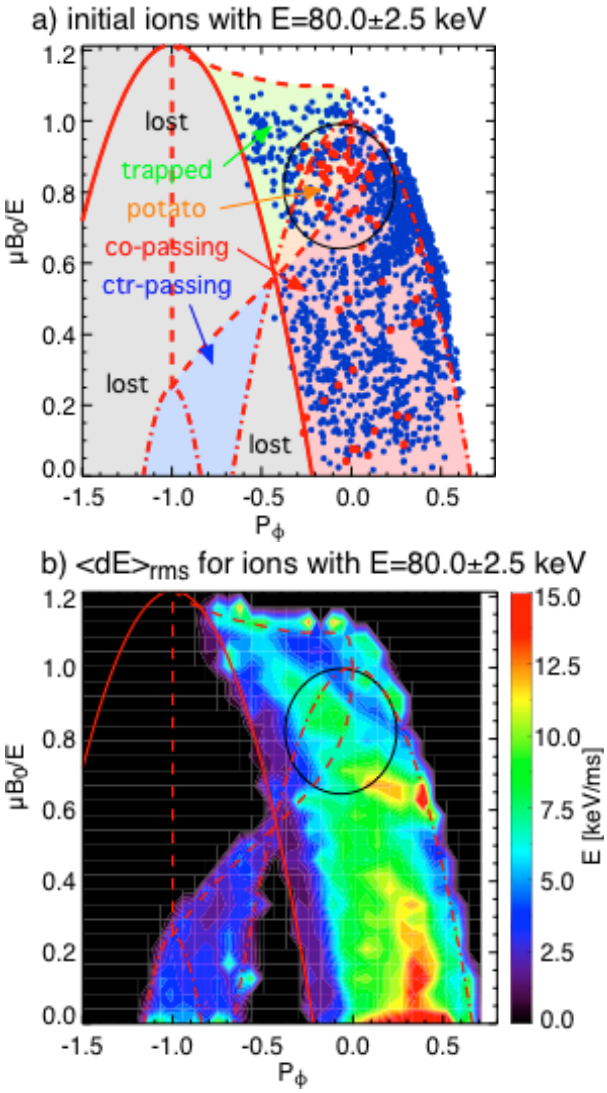

Fig. 10. a) Initial distribution of fast ions with 78.5 keV ≤ E_0 ≤ 82.5 keV - those in red are lost, b) rms fluctuation in energy for isotropic distribution of fast ions; stronger fluctuations (red) indicate stronger interaction with the modes.

ions have with the mode, that is, ions in the 'red' regions are more strongly resonant with the mode. No distinction is made between energy loss or gain which corresponds to drive and damping. This 'resonance' map can be compared to the initial fast ion distribution in the same energy range in Fig. 10a. The points in red are fast ions that are lost in the course of the simulation and come from wide range of initial parameters. A cluster of lost fast ions is circled in black (Fig. 10a) and that location is indicated by the black circle in Fig. 10b. Also shown by the red lines are the boundaries between

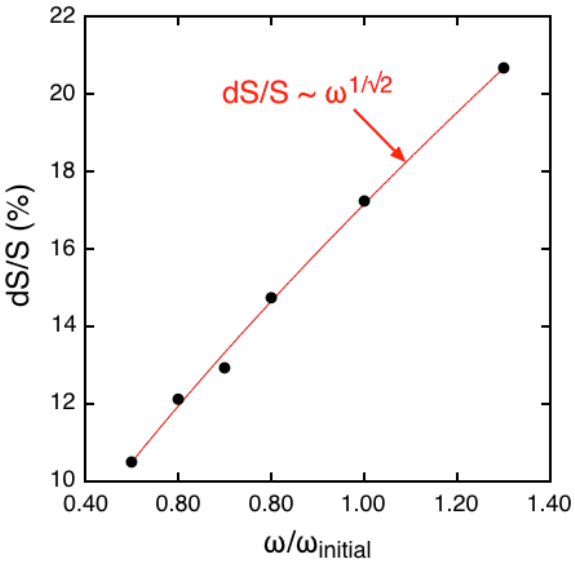

Fig. 11. Total neutron rate drop vs. scaled TAE amplitude (red squares), for the confined fast ion population (green diamonds) and due only to fast ion losses (blue circles).

different types of fast ion orbits, (trapped, co-passing, ctr-passing and potato).

The chirping of the mode frequency is curious. If the chirping is the result of the mode frequency "following" the evolution of a perturbation in the fast ion phase space [9], the NOVA-ORBIT approach used here is unlikely to be able to capture that subtle physics. Additional ORBIT simulations were done with a range of fixed frequencies for the modes. The frequencies were scaled from the onset frequency of each of the modes. In Fig. 11 is shown the simulated change in neutron rate vs. the scale factor for the initial frequency. The predicted neutron rate drop is larger using constant, initial frequency and has a slightly weaker than linear dependence on the scaled frequencies.

4. Summary

Significant drops in the neutron rate (and Da spikes) are seen correlated with strong bursts of multiple TAE. The data appear to be consistent with an avalanche-type process where the phase-space interactions of the multiple modes and resonances begin to overlap, resulting in a large enhancement in phase-space transport. Simulations of TAE structure with NOVA and fast ion transport with ORBIT find reasonable agreement with the experimental measurements.

The mode wave numbers are measured with an array of Mirnov coils and an array of fixed frequency reflectometers is used to measure the internal amplitude and radial profile of the modes. With this information, and the equilibrium reconstructions, perturbations to the fast ion transport due to the TAE are simulated with the linear NOVA ideal stability code, and the ORBIT guiding center particle tracking code. In the ORBIT simulations ≈50% of the neutron drop is due to transfer of energy from the fast ion population to the TAE, ≈40% of the drop from redistribution of the fast ions and the remaining 10% of the drop is due to actual losses of fast ions.

While ORBIT and NOVA do not self-consistently model the mode growth and fast ion transport, it might be assumed that the energy lost from the fast-ion distribution would transfer to the TAE. An estimate of the wave energy in the TAE burst is comparable to the decrement of energy in the fast-ion population at the observed mode amplitude.

5. Acknowledgements

The authors are grateful to the NSTX team for supporting these experiments. Work supported by U.S. DOE Contracts DE-AC02-76CH03073, DE-FG03-99ER54527, DE-FG02-06ER54867, and DE-FG02-99ER54527.

6. Bibliography

[1] ONO, M., et al., "Exploration of spherical torus physics in the NSTX device", Nucl. Fusion **40** (2000) 557.

[2] BERK, H. L., *et al*., "*Numerical simulation of bump-on-tail instability with source and sink*", Phys. Plasmas **2** (1995) 3007.

[3] GERHARDT, S. P., *et al., Calculation of the non-inductive current profile in high-performance NSTX plasmas,* Nucl. Fusion **51** (2011) 033004.

[4] FREDRICKSON, E. D., *et al*., "*Modeling fast-ion transport during toroidal Alfvén eigenmode avalanches in National Spherical Torus Experiment*", Phys. Plasmas **16** (2009) 122505.

[5] WHITE, R. B. and Chance, M. S., Phys. Fluids **27**, 2455 (1984)

[6] CHENG, C. Z., "*Kinetic Extensions of Magnetohydrodynamic Models for Axisymmetric Toroidal Plasmas"*, Phys. Reports (A Review Sec. of Phys. Letters.), **211**, 1-51 (February, 1992).

[7] KRAMER, G. J., *et al.,* "*Interpretation of core localized Alfvén eigenmodes in DIII-D and Joint European Torus reversed magnetic shear plasmas"*, Phys. Plasmas **13** (2006) 056104.

[8] CAROLIPIO, E M, *et al*., "*The toroidicity-induced Alfvén eigenmode structure in DIII-D: Implications of soft x-ray and beam-ion loss data*", Phys. Plasmas **8** (2001) 3391.

[9] BERK, H.L., *et al*., "*Spontaneous hole–clump pair creation*", Phys. Plasmas **6** (1999) 3102.